MSAS – Assignment #2: Modeling

Marcello Mutti, 220252

Exercise 1

The rocket engine in Figure 1 is fired in laboratory conditions. With reference to Figure 1, the nozzle is made up of an inner lining (k_1), an inner layer having specific heat c_2 and high conductivity k_2, an insulating layer having specific heat c_4 and low conductivity k_4, and an outer coating (k_5). The interface between the conductor and the insulator layers has thermal conductivity k_3.

1.1) Part 1: Parameters definition

Select the materials of which the nozzle is made of , and therefore determine the values of k_i ($i = 1, \dots, 5$), c_2, and c_4. Assign also the values of ℓ_i (i=1,...,5), L, and A in Figure 1.

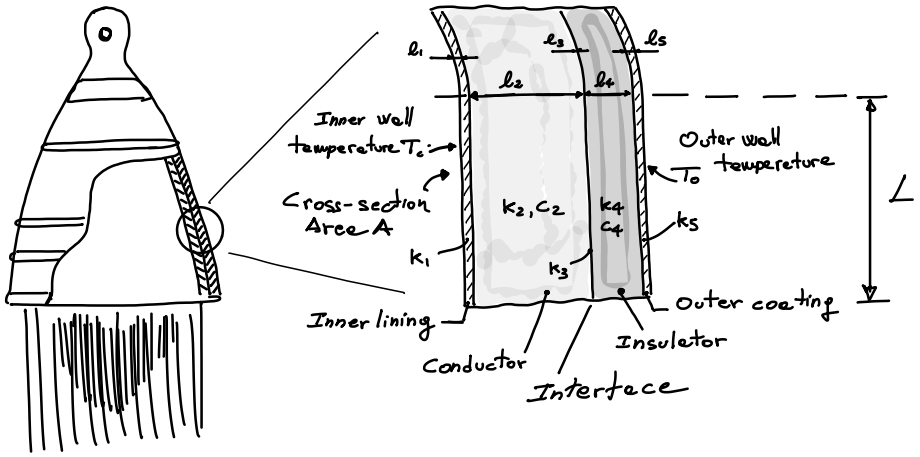

Figure 1: Real thermal system.

1.2) Part 2: Causal modeling

Derive a physical model and the associated mathematical model using one node per each of the five layers and considering that only the conductor and insulator layers have thermal capacitance. The inner wall temperature, T_i, as well as the outer wall temperature, T_o, are assigned. Using the mathematical model, carry out a dynamic simulation in MATLAB to show the temperature profiles across the different sections. At initial time, $T_i(t_0) = T_o(t) = 20$ C°. When the rocket is fired, $T_i(t) = 1000$ C°, $t \in [t_1, t_f]$, following a ramp profile in $[t_0, t_1]$. Integrate the system using $t_1 = 1$ s and $t_f = 60$ s.

1.3) Part 3: Acausal modeling

a) Reproduce in Simscape the physical model derived in Part 2. Run the simulation from $t_0 = 0$ s to $t_f = 60$ s and show the temperature profiles across the different sections. Compare the results with the ones obtained in point 1.2). b) Which solver would you choose? Justify the selection based on the knowledge acquired from the first part of the course. c) Repeat the simulation in Simscape implementing two nodes for the conductor and insulator layers and show the temperature profiles across the different sections.

(15 points)

1.1) For the inner lining, the selection of a Tungsten-Rhenium alloy W-3%Re was based on the alloy exceptional thermal resistance. The conductor layer is crafted from a Copper-based alloy, specifically GRCop-84, chosen for its combined high conductivity and mechanical strength. Both W-3%Re and GRCop-84 exhibit higher melting points compared to the anticipated inner wall temperature T_i.
The interface between the conductor and insulator layers incorporates a thin air gap, allowing exclusively conduction, thereby functioning as an insulating layer due to the low conduction coefficient λ of air. To further insulate the outer wall from the internal hot stream, a layer of Yttria-stabilized Zirconia 18YSZ is introduced. The outer coating is composed of 304 Stainless Steel, selected for its mechanical properties, as well as thermal and corrosion resistance.

Node n_i	Material	Conductivity $\lambda\,[W/m\,K]$	Specific Heat $c_p\,[J/kg\,K]$	Density $\rho\,[kg/m^3]\}$	Thickness $l\,[mm]$
1	W-3%Re [1]	115	-	-	5
2	GRCop-84 [2]	284	381.8	8810	20
3	Air	55×10^{-3}	-	-	0.1
4	18YSZ [3]	1.75	495	6047	7
5	SS3040 [4]	15.2	-	-	5

The nozzle itself is modeled as a truncated cone, defined by throat diameter $D_t = 17.2\,mm$, exit diameter $D_e = 312.7\,mm$ and divergent section length $L = 568.1\,mm$. Therefore, the total internal surface area:

$$A = L\frac{\pi\,(D_t + D_e)}{2} + \pi\left[\left(\frac{D_t}{2}\right)^2 + \left(\frac{D_e}{2}\right)^2\right] = 0.3839\,m^2$$

1.2) The heat flux between two generic nodes n_i and n_j can be modeled exploiting electrical similarity as:

$$Q = \frac{T_i - T_j}{R} \quad \text{with} \quad R = \frac{l}{kA}$$

The heat absorbed by the mass capacitive elements:

$$Q = C\frac{dT}{dt} \quad \text{with} \quad C = c_p m$$

The heat flow is assumed to be one directional, happening in particular in the radial direction of the nozzle. Given the symmetry of the problem, the cross area of the flow is taken as the internal side area A of the nozzle, and the the flow simplified as planar.
The heat exchange is conductive only, each layer subjected to the boundary conditions defined by the adjacent layers, or the wall temperature constraints T_i or T_0.

Therefore, modeling one node n_i per each layer, and assuming the node to be positioned at half the thickness of the respective layer l_i, the physical model can simply be derived as the combined in series effect of the resistive elements, with the additional lumped contribution of the heat storage effect due to the conductor and insulator layers.

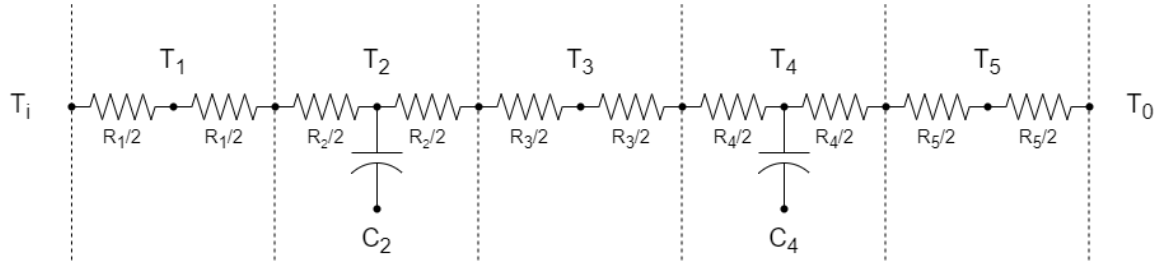

Figure 2: Physical model.

Node n_i	1	2	3	4	5
Resistance $R\,[K/W]$	1.13×10^{-4}	1.83×10^{-4}	4.74×10^{-3}	1.04×10^{-2}	8.57×10^{-4}
Capacity $C\,[J/K]$	-	2.58×10^{4}	-	8.04×10^{3}	-

It ought to be noted that given the 1D simplification, the masses m_i associated to the capacities are computed as $m_i = \rho_i A l_i$.

Given the boundary conditions $T_i\,(t)$ and T_0, the following Ordinary Differential Equations are derived from the physical model for n_2 and n_4:

$$\begin{cases} \dot{T}_2 &= \dfrac{1}{C_2}\left[-\left(\dfrac{1}{R_1+R_2/2}+\dfrac{1}{R_2/2+R_3+R_4/2}\right)T_2+\right. \\ &\quad \left.+\left(\dfrac{1}{R_2/2+R_3+R_4/2}\right)T_4+\left(\dfrac{1}{R_1+R_2/2}\right)T_i\right] \\ \dot{T}_4 &= \dfrac{1}{C_4}\left[\left(\dfrac{1}{R_2/2+R_3+R_4/2}\right)T_2-\left(\dfrac{1}{R_2/2+R_3+R_4/2}+\dfrac{1}{R_4/2+R_5}\right)T_4+\right. \\ &\quad \left.+\left(\dfrac{1}{R_4/2+R_5}\right)\right]T_0 \end{cases}$$

Noticeably the system is linear, and can therefore be written as:

$$\begin{pmatrix}\dot{T}_2\\ \dot{T}_4\end{pmatrix} = A_T\begin{pmatrix}T_2\\ T_4\end{pmatrix} + B_T\begin{pmatrix}T_i\\ T_0\end{pmatrix}$$

The matrices A_T and B_T defined as:

$$A_T = \begin{bmatrix} -\dfrac{\left(R_1+\frac{R_2}{2}\right)^{-1}+\left(\frac{R_2}{2}+R_3+\frac{R_4}{2}\right)^{-1}}{C_2} & \dfrac{\left(\frac{R_2}{2}+R_3+\frac{R_4}{2}\right)^{-1}}{C_2} \\ \dfrac{\left(\frac{R_2}{2}+R_3+\frac{R_4}{2}\right)^{-1}}{C_4} & -\dfrac{\left(\frac{R_2}{2}+R_3+\frac{R_4}{2}\right)^{-1}+\left(\frac{R_4}{2}+R_5\right)^{-1}}{C_4} \end{bmatrix}$$

$$B_T = \begin{bmatrix} \dfrac{\left(R_1+\frac{R_2}{2}\right)^{-1}}{C_2} & 0 \\ 0 & \dfrac{\left(\frac{R_4}{2}+R_5\right)^{-1}}{C_4} \end{bmatrix}$$

Given the linearity of the system, in order to chose the appropriate integration method it's possible to evaluate its eigenvalues:

$$\begin{Bmatrix} \lambda_1 \\ \lambda_2 \end{Bmatrix} = eig\left(A_T\right) = \begin{Bmatrix} -0.193\,06 \\ -0.032\,58 \end{Bmatrix}$$

Firstly it's worth noticing that the system is asymptotically stable. It's dominating dynamic is expected to be characterized by settling time $\tau \approx 4.6/\left|\lambda_2\right| \approx 141\,s$, therefore the system is expected to not have reached steady state conditions at t_f.
Furthermore, it is due to point out that indeed the eigenvalues are in different orders of magnitude, however the system is not considered as stiff:

$$\frac{|\lambda_1|}{|\lambda_2|} = 5.93$$

Therefore, given the simple dynamics of the system, MatLab's explicit Runge-Kutta integrator `ode45` is deemed capable of correctly capturing its behaviour. It ought to be noted that the time grid for the integration is constrained to the one defined by the solver of choice of the acausal model.

Using T_0 as initial condition for both nodes, T_2 and T_4 are propagated over the prescribed time interval. The temperatures associated to the remaining nodes are then computed according to the following algebraic equations:

$$\begin{cases} T_1 = \dfrac{R_1}{2}\left[\left(\dfrac{2}{R_1} - \dfrac{1}{R_1 + R_2/2}\right)T_i + \left(\dfrac{1}{R_1 + R_2/2}\right)T_2\right] \\ T_3 = \dfrac{R_2 + R_3}{2}\left[\left(\dfrac{2}{R_2 + R_3} - \dfrac{1}{R_2/2 + R_3 + R_4/2}\right)T_2 + \left(\dfrac{1}{R_2/2 + R_3 + R_4/2}\right)T_4\right] \\ T_5 = \dfrac{R_5}{2}\left[\left(\dfrac{2}{R_5} - \dfrac{1}{R_4/2 + R_5}\right)T_0 + \left(\dfrac{1}{R_4/2 + R_5}\right)T_4\right] \end{cases}$$

Below the results associated to the causal model:

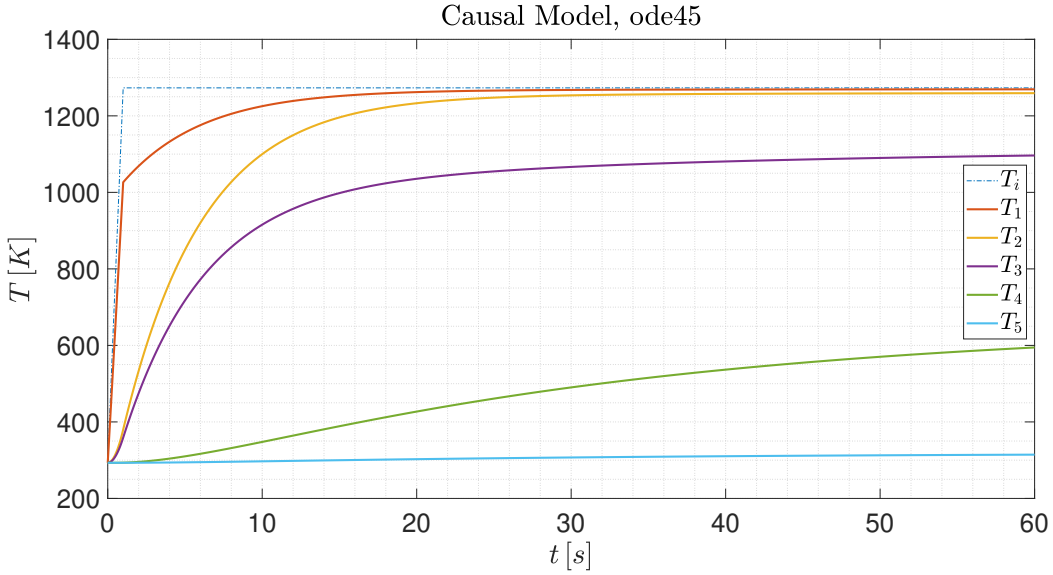

Figure 3: Nodal temperature profiles, causal model.

1.3) a) The physical model previously defined is used as basis for the creation of the Simscape acausal model. The resistances are modeled using thermal resistance blocks initialized with temperature gradient of $0K$. The masses are modeled using thermal masses of initial temperature T_0. The boundary conditions T_i and T_0 are set using a controlled thermal termal source and a constant thermal source respectively.
Below the temperature profiles:

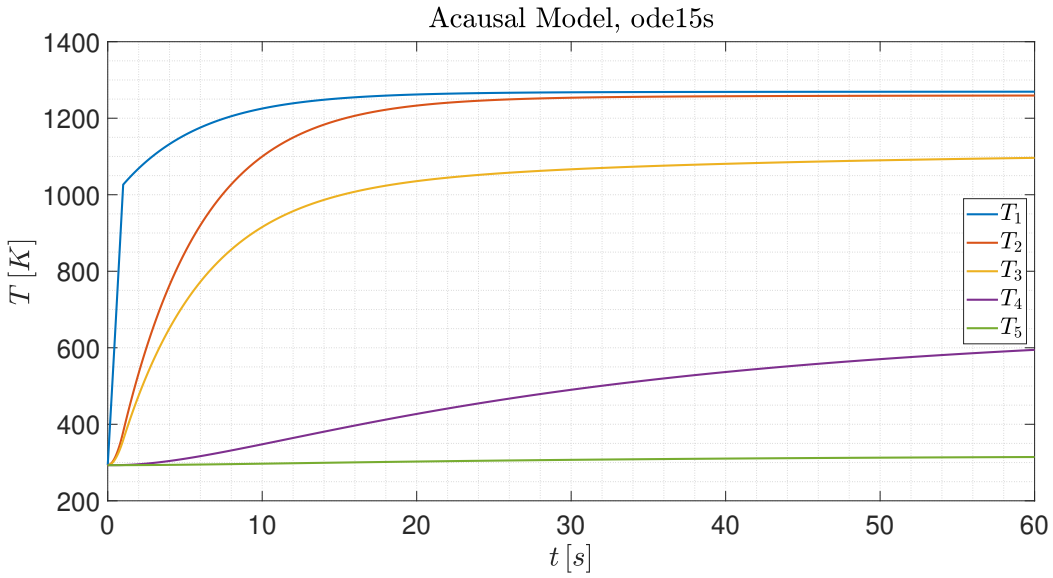

Figure 4: Nodal temperature profiles, acasual model.

In order to better visualize the difference between the two models the absolute displacement between $T_{i,c}$ (causal) and $T_{i,a}$ (acausal) is presented:

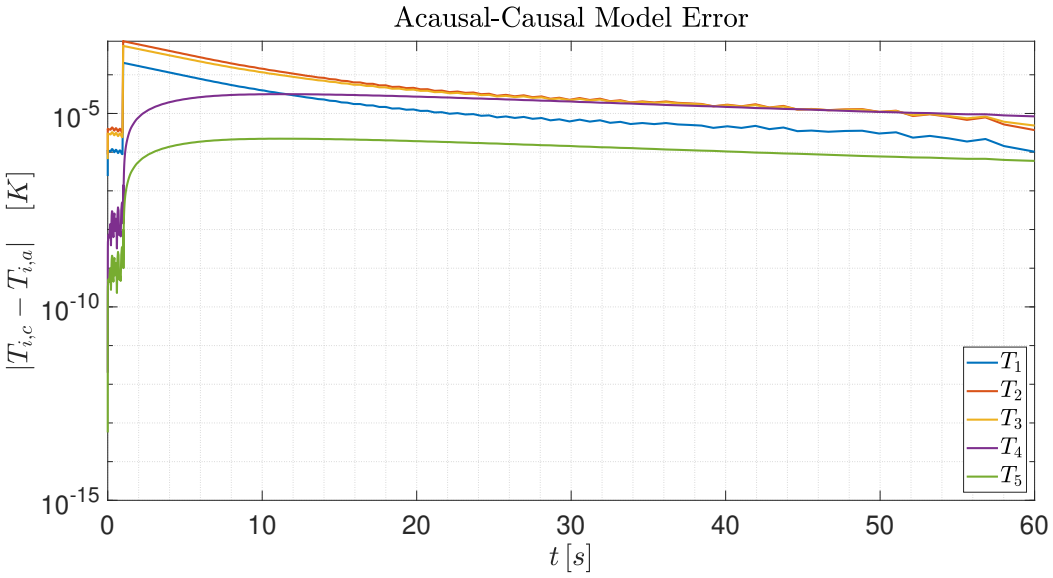

Figure 5: Acausal-Causal model comparison.

It ought to be noted that such plot is the result of the simulation of the 1-node model only, meaning that the 2-nodes model had been temporarily disabled. If the two acausal models are simulated in parallel the time grid is different.

b) In the Simscape environment all equations associated to the nodal temperatures are propagated in time simultaneously. The system is therefore characterized by Differential Algebraic Equations, and the choice of integration scheme constrained. For the sake of consistency, and in order to allow comparison between the two models, it was chosen to employ a scheme of equal order to `ode45`, therefore `ode15s` is chosen over `ode23t`.

c) The model is altered to account for one additional node for both the conductor and insulator layers. For consistency, it was again chosen to compute the temperature of the layer at half of its thickness.
The capacitive elements C_i, for $i = 2, 4$, are now split into two lumped masses of capacity $C_i/2$, located at one third and two thirds of the layer thickness.
The rest of the model is unaltered, together with the choice of integration scheme.

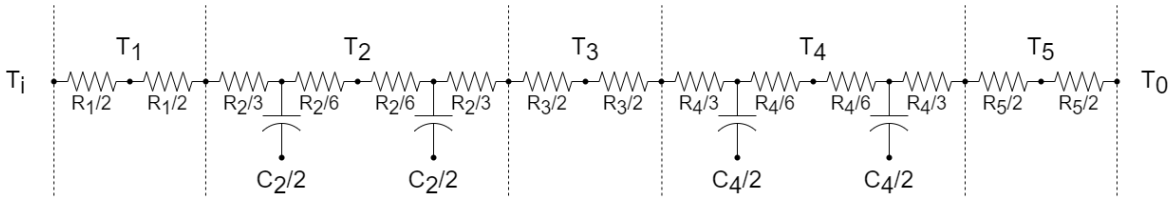

Figure 6: Physical model.

Below, the comparison between the 1-node acausal model against the 2-nodes one:

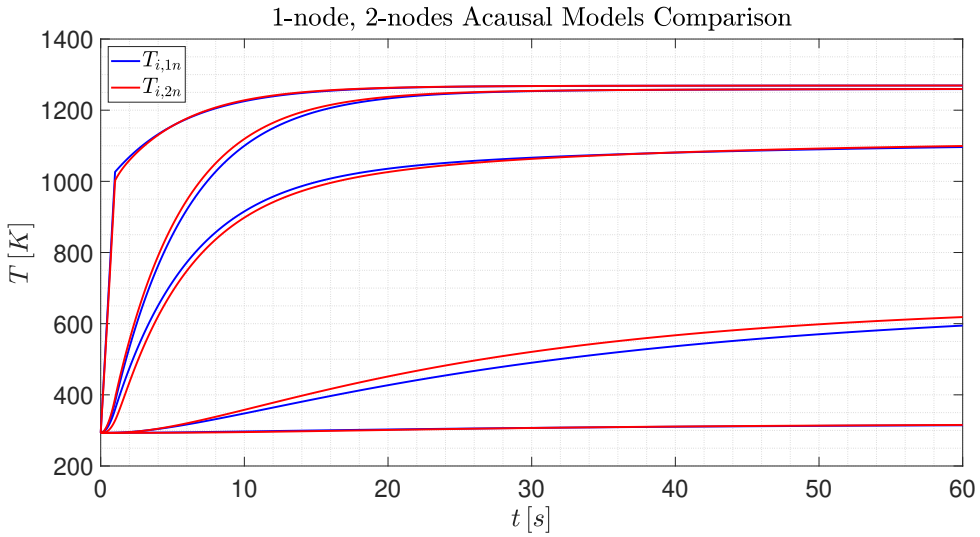

Figure 7: 1-node vs 2-nodes acasual models temperature profiles.

As the number of lumped parameters increases, the model becomes more representative of reality mostly in regards of the transient phase: at state conditions the mid-wall temperature of the layers is expected to converge to a common asymptotic value. Specifically, in the case of the comparison between 1 and 2 nodes, it is possible to observe that layers characterized by high thermal conductance will manifest noticeable differences in the first seconds of the simulation, but at time $t = 60\,s$ $|\Delta T| = |T_{1n} - T_{2n}|$ settles below the threshold of $|\Delta T| < 5\,K$.
The insulator layer, characterized by high thermal inertia and associated to the longer system transient, manifests a more significant displacement over time. However, given a long enough simulation time t_f, it is again expected to reach convergence in terms of $|\Delta T|$.

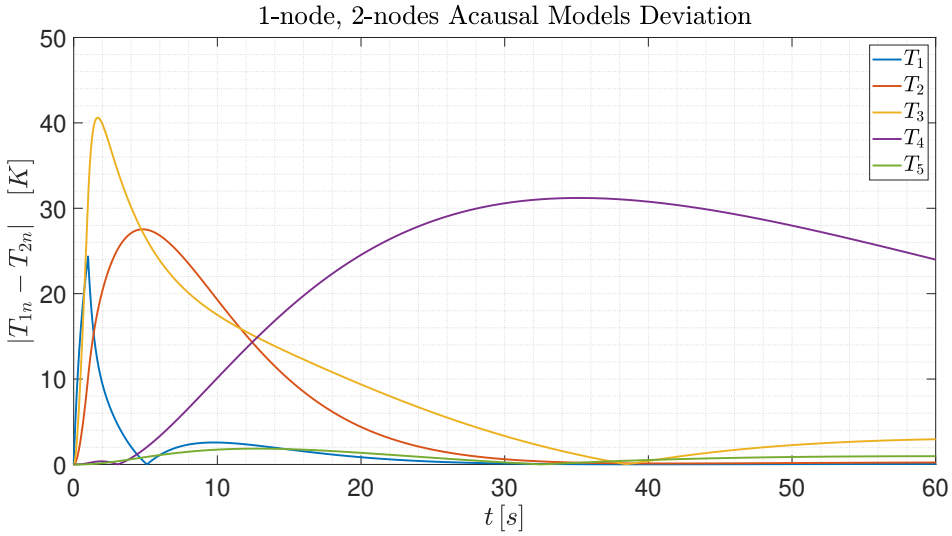

Figure 8: 1-node vs 2-nodes acasual models temperature profiles.

Exercise 2

The real system of an electric propeller engine is depicted in Figure 9. It is composed by a DC permanent magnet motor which drives a propeller shaft. Between the motor and propeller shaft there is a single stage gear box to regulate the angular speed ratio. Moreover, to avoid overheating of the gear unit, the system is augmented by a cooling system where a fluid exchanges heat with the gear box itself. In Figure 10 a functional breakdown structure of the system is shown.

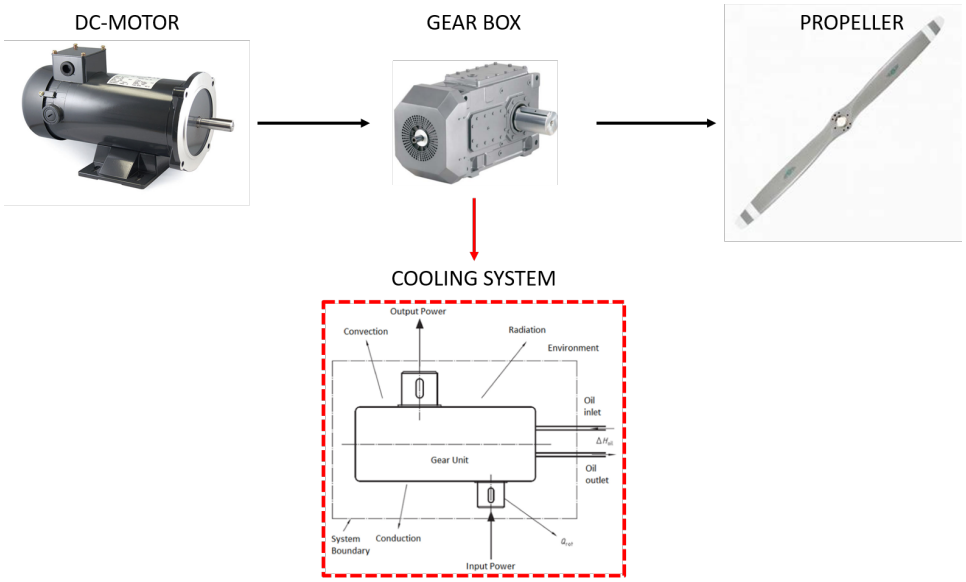

Figure 9: Real system.

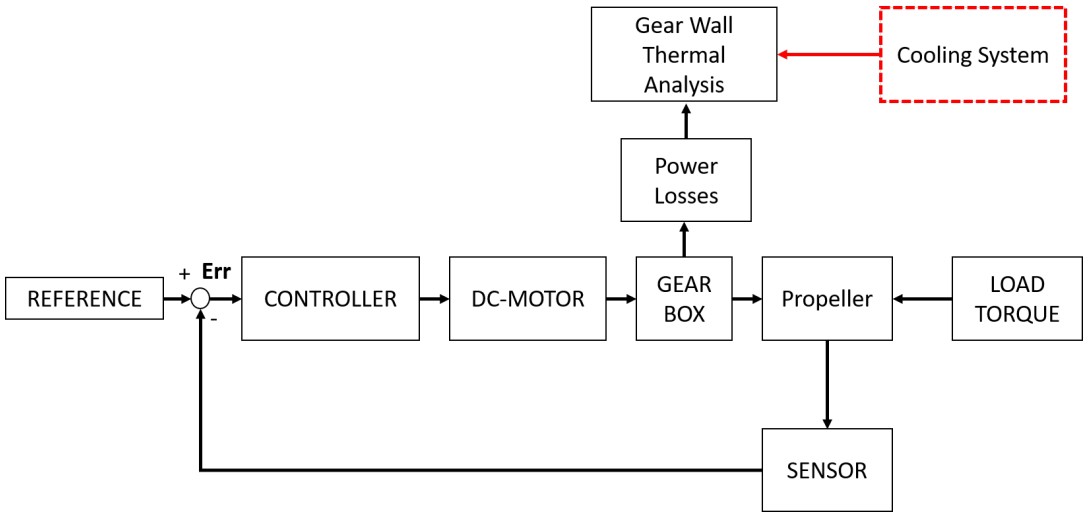

Figure 10: Functional block scheme of the system.

2.1) Part 1: Propeller Electric Engine

Considering the real system in 9 **without** the cooling part, you are asked to:

1. Extract a physical model highlighting assumptions and simplifications.
2. Reproduce the model in acausal manner in Dymola.

3. According to the block scheme in 10, tune a controller (e.g., a PID controller) such that the motor input voltage remains less than 200 V and the error signal **Err** is less than 0.1 rad/s after 10 s.

4. Study the Gear box temperature and heat flux for a simulation time of $\mathbf{t_f} = 120$ s (considering only conduction as heat transfer).

5. Discuss the simulation results and the integration scheme used

For the simulation part, you shall consider: the DC motor data listed in Table 1; the gear box data listed in Table 2, with loss parameters in Table 3; a propeller made of **aluminium** with nominal angular speed $\hat{\omega}$ and a nominal quadratic speed load torque $\hat{T}_{load}$ acting on it (Table 4). The reference angular speed signal to be tracked by the propeller is given in Figure 11.

Table 1: DC motor data

Parameter	Value	Unit
Coil Resistance	0.1	Ω
Inductance	0.01	H
Motor Inertia	0.001	kg m^2
Motor Constant	0.3	Nm/A

Table 2: Gear Box data

Parameter	Value	Unit
Mass	3	kg
Gear ratio	2	[-]
Specific heat	1000	J/(kg K)
Thermal Conductivity	100	W/K

Table 3: Gear Box Loss Table

Driver angular speed [rad/s]	Mesh efficiency[-]	Bearing friction torque [Nm]
0	0.99	0
50	0.98	0.5
100	0.97	1
210	0.96	1.5

Table 4: Propeller data

Parameter	Value	Unit
Diameter	0.8	m
Thickness	0.01	m
$\hat{\omega}$	210	rad/s
$\hat{T}_{load}$	100	Nm

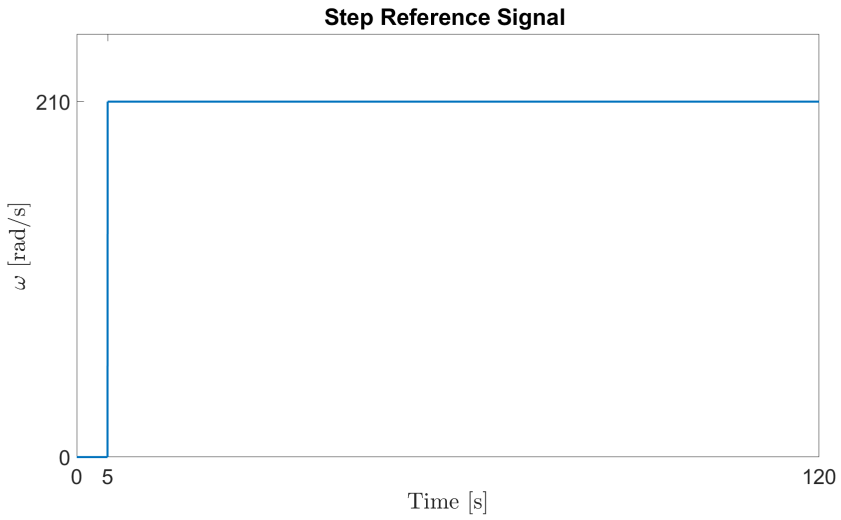

Figure 11: Angular speed reference for the propeller.

2.2) Part 2: Cooling System

After the previous gear unit thermal analysis, now consider the steady-state condition reached by the propeller engine at the end of the simulation to model and simulate a single **fixed** volume flow rate cooling system (as shown in Figure 9) for the gear unit and considering only **convection** as heat transfer. In particular, you are asked to:

1. Derive a physical model highlighting assumptions and simplifications.
2. Reproduce the acausal model in Dymola.
3. Tune the cooling system in terms of volume flow rate, control logics, and initial fluid storage temperature such that:
   (a) the gear unit is kept between 40°C and 60°C.
   (b) the source tank does not get empty before the end simulation time
   (c) the storage tanks have a maximum height of 0.8 m and cross section area of 0.01 m^2
   (d) the system shall have a recirculating capability in order to exploit the outlet fluid for a next cooling process (when the source tank get empty)
   (e) the sink heated fluid is kept between 5°C and 10°C.
   (f) the power consumption of the thermal system shall be no more than 6 kW
4. Discuss the simulation results and the integration scheme used

For the simulation part consider properties of water at 10°C as cooling incompressible fluid (convective thermal conductance $\lambda_{conv} = 300$ W/K) and the cylindrical pipe line data listed in Table 5. The simulation shall last at least $\mathbf{t_{sim}} = 300$ s starting with no water along the pipe.

Table 5: Pipe line properties

Parameter	Value	Unit
Diameter	4	cm
Length	40	cm
Geodetic height	0	m
Friction losses	0	[-]

(15 points)

2.1.1) As per the functional block breakdown of the system, the entire apparatus can be simply constructed by interfacing the individual subsystems.

The DC motor is modeled on the basis of a brushed DC motor.
It is therefore characterized by an ideal generator of input voltage V_{in}, the resistance R_c and the inductance L_c associated to the coil windings. The circuit is affected by an additional voltage drop V_e due to the counter electromotive force associated to the magnetic self inductance effect. The brushed rotor is assumed to be frictionless and characterized inertia J_m defined in Table 1.
The power transformation is defined by the motor torque constant k_T according to the equations:

$$\begin{cases} V_e I = T_m \omega_m \\ k_T = \dfrac{T_m}{I} \end{cases}$$

The electrical losses due to Joule effect do not contribute in the heating up of the gear box.

The gear box power losses are modeled as friction dissipation. The heat generated is transferred by means of conduction only, and stored in the gear box walls of external measured temperature T_w.

The propeller shape is simplified to a square base aluminum parallelepiped. Given the basis dimensions $t = 0.01\,m$ and diameter $D = 0.8\,m$, assuming density of $\rho = 2710\,kg/m^3$, the propeller moment of inertia:

$$J_p = \frac{1}{12}\rho t^2 D\left(t^2 + D^2\right) \approx 0.01156\,kg\,m^2$$

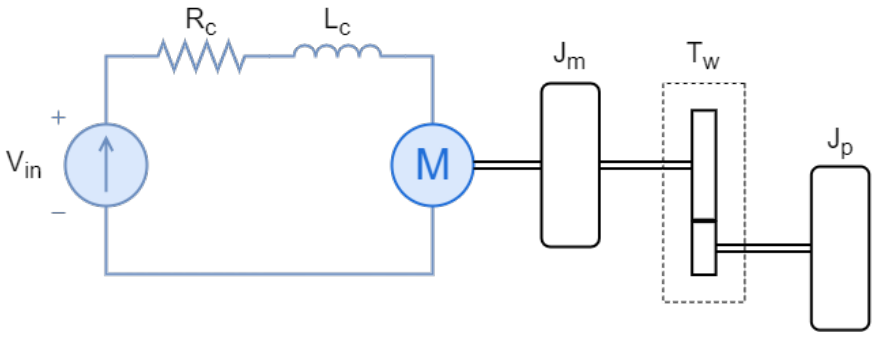

Figure 12: Electro-mechanical components.

The propeller is subjected to load torque function of the propeller drag. It is therefore assumed to be quadratic in the angular velocity of the propeller ω. The torque is constrained to be $T_{load} = 0\,Nm$ at $\omega = 0\,rad/s$, and $\hat{T}_{load}$ at $\hat{\omega}$.

The controller is a continuous Proportional-Integral (PI) controller. It outputs V_{in} as its control variable, given the input:

$$\epsilon_\omega = \omega_{ref} - \omega$$

The reference signal ω_{ref} is defined as per Fig. 11.

2.1.2) The acausal model is driven by reference angular velocity ω_{ref}.
The electrical components are initialized with $V_{in} = 0\,V$, $I = 0\,A$, while the mechanical components are initialized with $\omega = 0\,rad/s$.
The gear box wall has initial temperature of $T_{w,0} = 25°C$.

2.1.3) The PI controller is tuned according to Ziegler-Nichols method.
Both proportional gain k and integral time constant T_i have to be chosen to guarantee system convergence in the prescribed settling time. In particular T_i plays a crucial role in terms of steady state convergence. Below the chosen PI parameters:

k	=	0.03
T_i	=	$0.025\,s$

The input and output values ϵ_ω and V_{in} respectively:

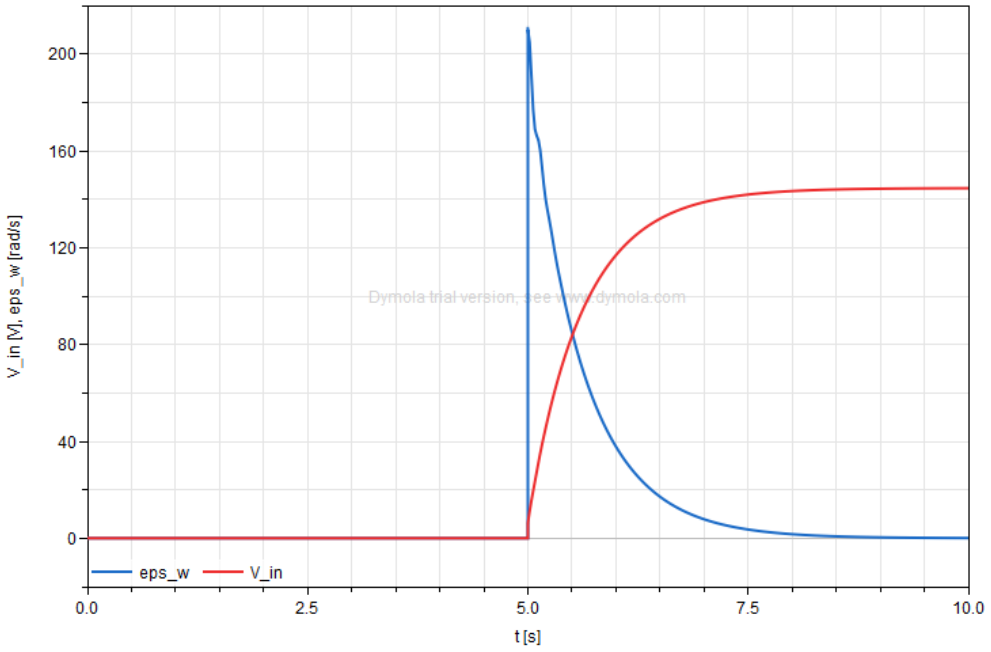

Figure 13: Input voltage V_{in} and angular velocity error ϵ_ω time evolution.

At $t = 10\,s$:

$V_{in}\,(t = 10\,s)$	=	$144.52591\,V$
$\epsilon_\omega\,(t = 10\,s)$	=	$0.07663942\,rad/s$

2.1.4) Without cooling system, the gear box temperature is to increase indefinitely in function of time. The temperature profile is expected to be linear once the system reaches steady state conditions.

The wall temperature T_w and heat flow rate Q at $t = 120\,s$ are used as starting conditions for the simulation of the cooling system:

$T_w\,(t = 120\,s)$	=	$116.7369\,°C$
$Q\,(t = 120\,s)$	=	$2414.4927\,W$

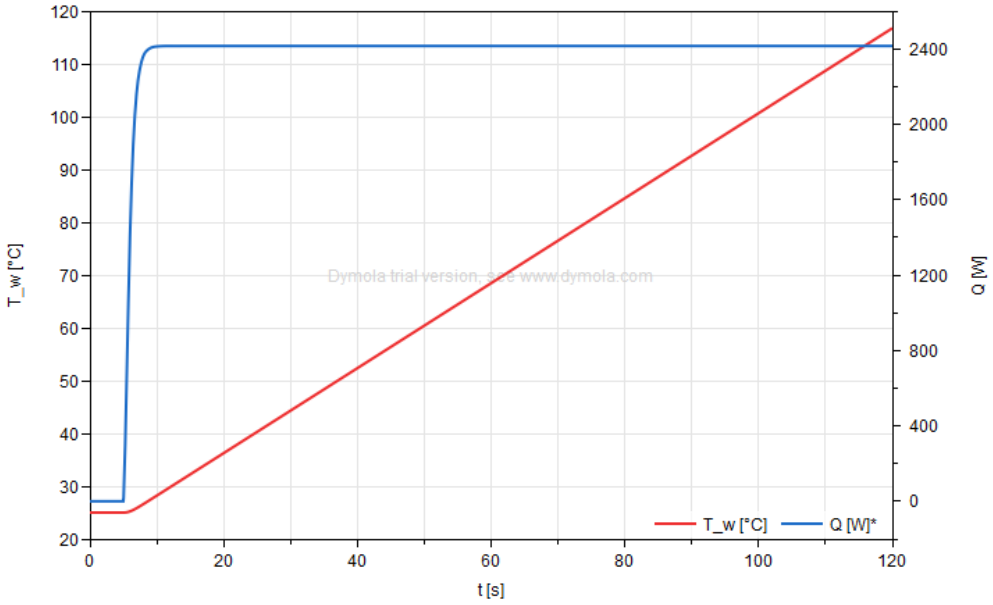

Figure 14: Temperature wall T_w and dissipated heat flow rate Q time evolution.

The overall system steady state conditions:

Ideal Generator	$V_{in} = 144.58\,V$	$I = 185.83\,A$	$P_{in} \approx 26917.92\,W$
Electrical Motor	$T_m = 55.75\,Nm$	$\omega_m = 420.00\,rad/s$	$P_m \approx 23414.49\,W$
Gear Box Output	$T_p = 100.00\,Nm$	$\omega_p = 210.00\,rad/s$	$P_p \approx 21000.00\,W$
	Motor efficiency	$\eta_m = \dfrac{P_m}{P_{in}} = 87.15\%$	
	Gear box efficiency	$\eta_p = \dfrac{P_p}{P_m} = 89.69\%$	
	Global efficiency	$\eta_T = \dfrac{P_p}{P_{in}} = 78.16\%$	

2.1.5) The system is characterized by both electrical and mechanical dynamics. The time scales associated to these physicals domains are usually very different, therefore the system might be stiff.
The choice of integration schemes leans towards $\mathcal{A}$-stable methods or explicit methods. The DASSL scheme, based on Backwards Difference Formulae up to order 5, proves to be effective in the propagation.
Given the non-linearity of the system, it is meaningless to discuss stability in terms of eigenvalues. However, studying the behaviour of the poles of the linearized system at different time instants can be useful in terms of step size analysis.
In particular, it is found that for $t \in [0,\, 120]\ s$, the eigenvalue λ_i with lower $Re\{\lambda_i\}$ is found at steady state conditions as:

$$\widetilde{\lambda} \approx -36.55 \pm 39j \qquad \begin{cases} |\widetilde{\lambda}| \approx 53.45 \\ \phi_{\widetilde{\lambda}} \approx \pm 133.14^\circ \end{cases}$$

The remaining eigenvalues belong to the spectral circle defined by $\widetilde{\lambda}$, in particular with $Re\{\lambda_i\} \leq 0\ \forall t \leq 120\,s$.

For RK4, the maximum λh value associated to $\alpha = \phi_{\widetilde{\lambda}}$ is $(\lambda h)_{max} \approx 2.7$. Therefore the maximum step size:

$$h_{max} = \frac{|\lambda h|_{max}}{|\widetilde{\lambda}|} \approx 0.5$$

This assumption is verified by simulation experiments. RK4 with fixed step $h < h_{max}$ indeed converges to results similar to those of DASSL.

2.2.1) In order to model the cooling system, it is assumed that the electrical and mechanical subsystems have reached steady state conditions, so that the gear box is subjected to constant heat flow rate of $Q = 2414.4927\,W$.

The gear box is to be cooled using a convective heat exchanger with water as cooling liquid. The heat exchanger is assumed to be located on the gear box wall, with pipes of $0\,m$ geodetic height. The cooling liquid properties are taken at $T = 10°C$, $p = 1\,bar$ and assumed to be constant. The liquid is also considered incompressible and frictionless, therefore no pressure gradients are present along the pipe.

Both the source and sink tanks are assumed to be subjected to atmospheric pressure of $p_{amb} = 1\,atm$. In order to account for recirculating capability the heat exchanger output flow temperature has to be controlled. The heat to be removed by the sink tank is determined by a limited-output PI controller. This type of controller is chosen over a hysteresis switch one in order to avoid high frequency power cycles when the hot stream starts pouring into the empty sink tank.
The coolant flow is controlled via an ideal volumetric pump by a switch with thermal hysteresis. The pump is capable of providing constant prescribed flow rate, regardless of the pressure gradient across its ports. Such gradient is proportional to the level of the tanks.

2.2.2) The heat generated by the gear box losses is modeled as a prescribed heat flow source. The conductive element is added for completeness, but does not alter the results.
All hydraulic components are initialized at temperature $T_0 = 5°C$. The heat exchanger is modeled as a single pipe, initially empty.
The source tank is assumed to be 95% full, starting at a level of $0.76\,m$. The sink tank is initially empty as well, but for numerical reasons its initial level is set to an arbitrary low value, e.g. 10^{-15}.
The heat removed from the sink tank is modeled as a prescribed heat flow source.

2.2.3) In order the to keep the gear box between the assigned temperatures the activation threshold of the hysteresis switch is set to $58°C$, while the deactivation one is set to $42°C$. When active, the pump is set to allow a volumetric flow rate of $\dot{\overline{V}} = 2.5 \times 10^{-5}\,m^3/s$.
If the pump were to remain active for the whole duration of the simulation, the maximum allowed flow rate $\dot{V}_{max}$ would be:

$$\dot{V}_{max} = \frac{H_t A_t}{t_{sim}} = 2.5\overline{3} \times 10^{-5}\,m^3/s > \dot{\overline{V}}$$

The PI controller determines the heat flow to be removed from the sink tank given the tank temperature T_t and a reference temperature set to $T_{ref} = 7.5\,°C$. The controller parameters k and T_i are chosen so to quickly stabilize the temperature without exceeding the prescribed limits. The controller output Q_t is also limited to the $[-6,\, 0]\ kW$ interval.

2.2.4) Below the simulation results regarding gear box wall temperature T_w, sink tank temperature T_t and thermal system power consumption Q_t:

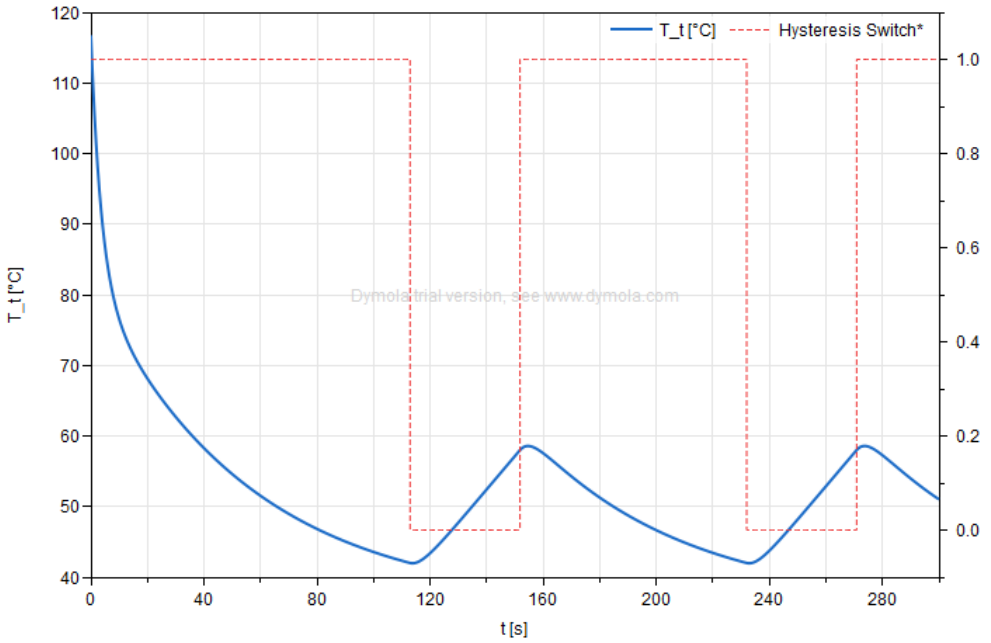

Figure 15: Gear box wall temperature T_w and hysteresis boolean switch state.

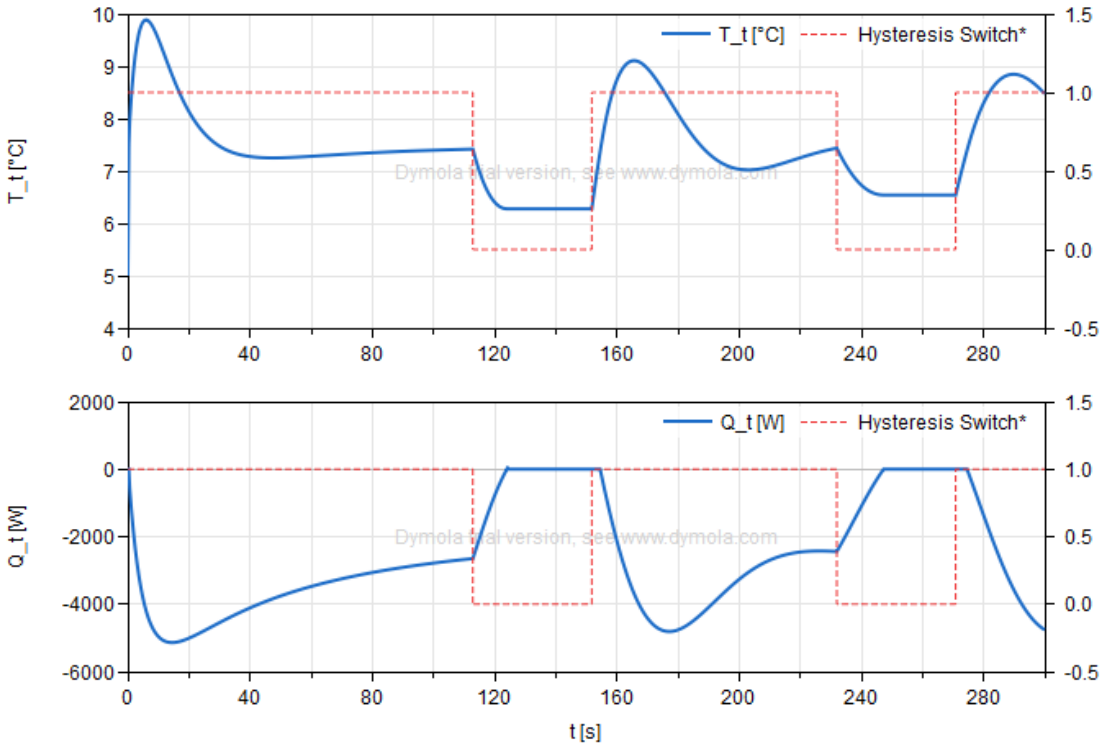

Figure 16: Sink tank temperature T_t, thermal power consumption Q_t and hysteresis boolean switch state.

The source and sink tanks level profiles:

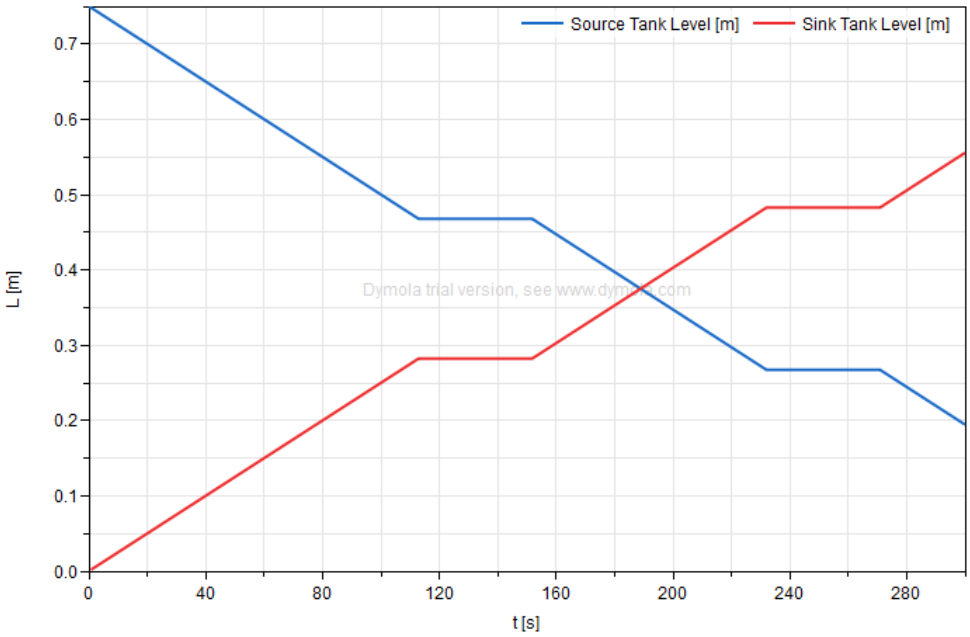

Figure 17: Tank levels.

Given that all the temperature requirements are satisfied, and given that the source tank is not emptied out at the end of the simulation, it is possible to affirm that a recirculating cooling system would be capable of adequately dispersing the gear box generated heat.

The results presented were again computed using DASSL integration scheme, which proves to provide the best results.
As per the previous simulation, the system is linearized over sampled time instants $t \in [0, 300]\ s$. It is found that the associated eigenvalues are always stable, and the furthest to the left the imaginary axis is the one of greater magnitude, and it is real $\overline{\lambda} \approx -0.274$. Given the stability constraint $|\lambda h|_{max} = 2.7853$, the maximum step size to achieve convergence in terms of RK4 integration scheme is $h_{max} \approx 10\,s$.
However, for high values of $h \leq h_{max}$ RK4 is incapable of correctly capturing the behaviour of T_t in the first seconds of the simulation, and builds up significant accumulation error. This is due to the fact that the sink tank is initially empty, so when water first starts flowing in its thermal inertia is extremely low and therefore extremely sensible to temperature variations.
For $h = 0.1$, the results yielded by the fixed step RK4 method are comparable to those of the variable step explicit DASSL.
Still, a variable step method is preferable in order to correctly capture the exact time instants associated to the switching dynamics.

References

[1] Makoto Fukuda, Akira Hasegawa, and Shuhei Nogami. "Thermal properties of pure tungsten and its alloys for fusion applications". In: *Fusion Engineering and Design* (2018). URL: https://www.sciencedirect.com/science/article/pii/S0920379618304113.

[2] Robert P Minneci et al. "Copper-based alloys for structural high-heat-flux applications: a review of development, properties, and performance of Cu-rich Cu-Cr-Nb alloys". In: *International Materials Reviews* (2021). URL: https://www.tandfonline.com/doi/full/10.1080/09506608.2020.1821485.

[3] Xiwen SONG et al. "High-temperature thermal properties of yttria fully stabilized zirconia ceramics". In: *Journal of Rare Earths* (2011). URL: https://www.sciencedirect.com/science/article/pii/S100207211060422X.

[4] *Material Properties: 304 Stainless*. URL: https://trc.nist.gov/cryogenics/materials/304Stainless/304Stainless_rev.htm (visited on 12/16/2023).